Journal of Alloys and Compounds 500 (2010) 34–38

Contents lists available at ScienceDirect

Journal of Alloys and Compounds

journal homepage: www.elsevier.com/locate/jallcom

Morphology investigation of yttrium aluminum garnet nano-powders prepared by a sol–gel combustion method

Kai Guo[a,b], Hao-Hong Chen[a], Xiangxin Guo[a], Xin-Xin Yang[a], Fang-Fang Xu[a], Jing-Tai Zhao[a,*]

[a] Key Laboratory of Transparent Opto-functional Inorganic Materials of Chinese Academy of Sciences, Shanghai Institute of Ceramics, 1295 Ding Xi Road, Shanghai 200050, PR China
[b] Graduate School of Chinese Academy of Sciences, 19A Yu quan Road, Beijing 100039, PR China

ARTICLE INFO

Article history:
Received 22 September 2009
Received in revised form 2 March 2010
Accepted 2 March 2010
Available online 9 March 2010

Keywords:
YAG nano-powder
Sol–gel combustion method
Chelating agent
Fuel
EDTA

ABSTRACT

Highly sinterable yttrium aluminum garnet (YAG) nano-powders have been synthesized by a sol–gel combustion method with various chelating agents and fuels, namely citric acid, tartaric acid, glycine and ethylene diamine tetraacetic acid (EDTA). The preparation involved the thermal decomposition of a chelating agent (fuel)–nitrate gel and the formation of amorphous precursors. The as-synthesized precursors were studied by infrared spectroscopy (IR), thermogravimetric (TG) and differential scanning calorimetric (DSC) analyses. The nano-powders calcined at 1000 °C were characterized by X-ray powder diffraction (XRD) and transmission electron microscopy (TEM). It was found that the chelating agents and fuels used had a significant influence on the average grain size and agglomeration of YAG nano-powders. The rate of combustion reaction between chelating agent (fuel) and nitrate was responsible for the growth of the grains. Nano-particles with the smallest size and high sinterability were obtained when using EDTA, which derived from the significant blocking of the diffusion path associated with the lowest combustion reaction rate.

1. Introduction

Due to its excellent optical properties, yttrium aluminum garnet ($Y_3Al_5O_{12}$ or YAG) is considered as an important solid-state laser material, phosphor and window materials for a variety of lamps [1–3]. Since Ikesue et al. found that transparent polycrystalline YAG had nearly the same optical characteristics as single crystal YAG, considerable efforts have been devoted to fabricating high-transmittance YAG ceramics [4]. For application purposes, one crucial point is to synthesize high-quality powders with good dispersity, sphere shaped and suitable particle size distribution. At present, preparation of YAG powders by standard solid-state reactions has been widely investigated and well developed from calcination temperatures, ball milling process and starting materials and so on [5–7]. However, the method has some disadvantages, i.e. the tedious mechanical mixing and the extensive heat treatments at high temperatures. This way, it is difficult to guarantee the purity and control the grain size of YAG powders [8]. Because of the uniform mixing of starting materials and the excellent chemical homogeneity of the final products, various wet-chemical routes have been proposed to lower the sintered temperature and eliminate the presence of intermediate phases. These include sol–gel [9,10], co-precipitation [11–13], spray pyrolysis [14], and combustion [15–19]. Among these preparation techniques, the sol–gel combustion method appears to be the simplest and least price, as proved by preparations of $SrTiO_3$ powders reported by Pechini in 1967 [20]. Other materials such as $SrO(SrTiO_3)_n$ [21], $CoFe_2O_4$ [22], TiO_2 [23], $MgFe_2O_4$ [24], have been synthesized following the same technique.

Because a significant number of surface atoms can cause a surface-quantum effect, the nanometer-size YAG particles can have higher sinterability [25]. Superfine YAG nano-powders have an important advantage for fabricating high-performance YAG transparent ceramics, especially when considering the good ability to control the grain boundaries [26,27]. The effect of various chelating agents and fuels on the grain size and agglomeration of YAG nano-powders by the sol–gel combustion method has been scarcely investigated. In the present paper, citric acid, tartaric acid, glycine, and EDTA were studied both as chelating agents during sol–gel process and as fuels in combustion reaction. The crystalline evolution was evaluated by infrared spectroscopy (IR), thermogravimetric (TG) and differential scanning calorimetric (DSC) analyses. The phase and morphology of the as-synthesized nano-powders were characterized by X-ray powder diffraction (XRD) and transmission electron microscopy (TEM), respectively. The influence of the organics used on the morphology of the nano-powders was discussed.

* Corresponding author. Tel.: +86 21 5241 2073; fax: +86 21 5241 3122.
E-mail address: jtzhao@mail.sic.ac.cn (J.-T. Zhao).

0925-8388/$ – see front matter © 2010 Elsevier B.V. All rights reserved.
doi:10.1016/j.jallcom.2010.03.037

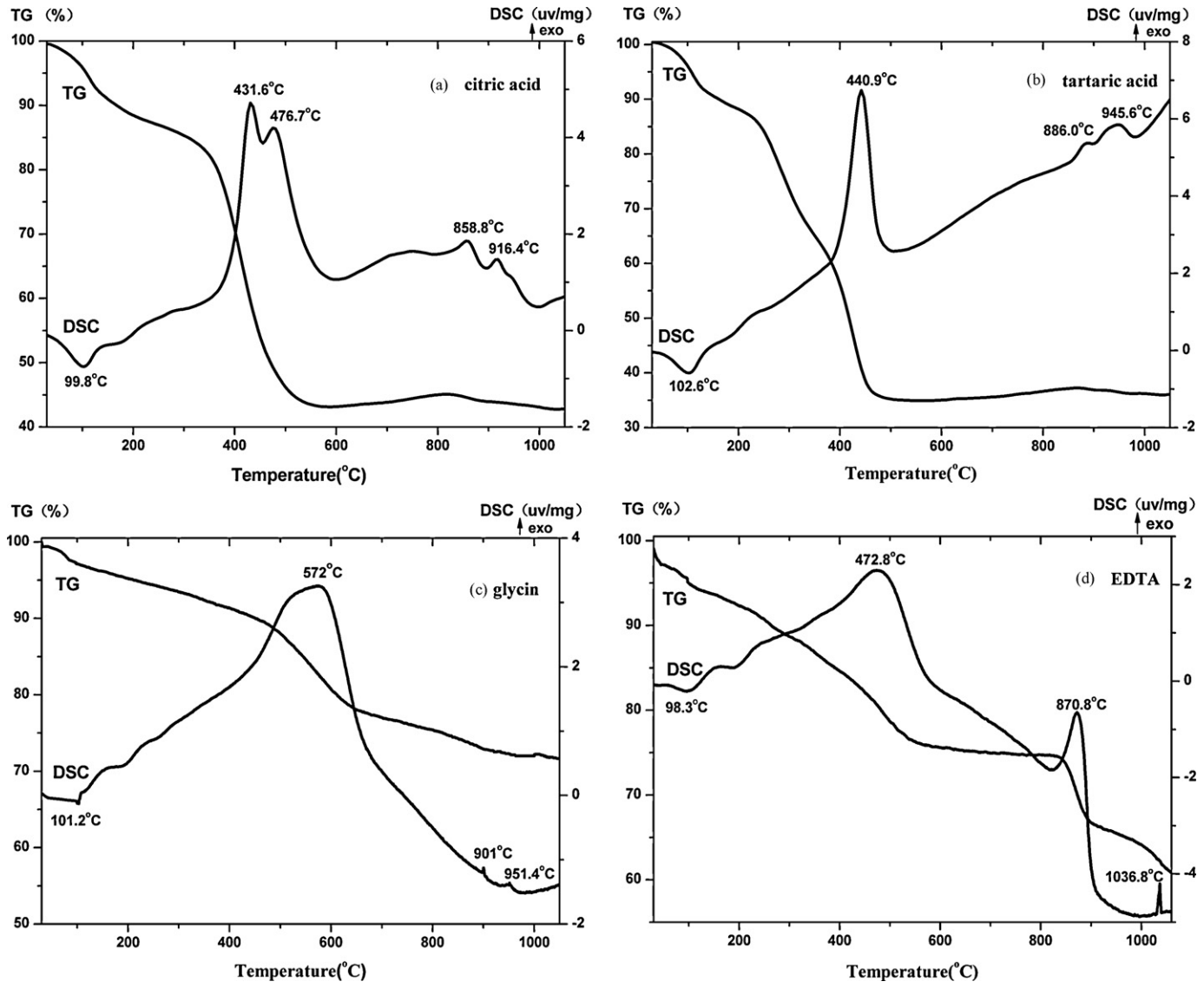

Fig. 1. TG–DSC curves of precursors: (a) citric acid; (b) tartaric acid; (c) glycine and (d) EDTA.

2. Experimental

2.1. Synthesis of YAG nano-powders

The synthesis of YAG nano-powders via the original or modified combustion method has been discussed in some references [19,28]. The modified sol–gel combustion method is a combination of the sol–gel method and the self-propagating high temperature synthesis (SHS) process [29]. Y_2O_3 (99.999%) and $Al(NO_3)_3{\cdot}9H_2O$ (A.R.) were used as starting materials. An aqueous nitrate solution of Y^{3+} was prepared by dissolving Y_2O_3 in diluted nitric acid (HNO_3, AR) under stirring at 60 °C for 2 h. The $Al(NO_3)_3$ solution was made by dissolving $Al(NO_3)_3{\cdot}9H_2O$ in deionized water. Both aluminum and yttrium solutions were mixed at a stoichiometric ratio of Y^{3+}:Al^{3+} = 3:5. After sonicated for 10 min, the chelating agent solution (citric acid/nitrite = 5:6, tartaric acid/nitrite = 3:2, glycine/nitrite = 5:3 or EDTA/nitrite = 3:8) was then added to the mixture and stirred for 2 h at 60 °C, pH ~3–4. Heating at 80 °C, the solution was converted to gel after the evaporation of some water. The gel was rapidly moved to the oven at 200 °C to start the auto-combustion process. The SHS process continued for only 1–3 min, and then fluffy precursors were obtained. Finally, the precursors were calcined at 1000 °C in a muffle furnace in air.

2.2. Characterization of the samples

TG/DSC analysis was done on a NETZSCH STA 409 PC/PG instrument. Measurements were taken under a continuous flow of air. The precursors were heated at a rate of 10 °C/min to 1100 °C and then cooled to ambient temperature in air. The XRD data for phase identification were collected at ambient temperature on a Huber G-670 diffractometer (Cu $K_{\alpha1}$ radiation, λ = 1.54056 Å, 40 kV/30 mA). The 2θ for all data ranged from 4° to 80° with 0.005° steps size. IR spectra of the samples were measured on a Nicolet NEXUS 7000C spectrophotometer in the range from 400 cm^{-1} to 4000 cm^{-1} using the KBr pellet (1 wt% sample) method. The particle size and morphology of the powders were examined on a transmission (TEM, JEOL, JEM 2100F), and the surface of YAG ceramics was examined on a scanning electronic microscope (SEM, LEO 1530).

3. Results and discussion

3.1. Thermal analysis

For comparison, TG–DSC analyses of the precursors with various chelating agents and fuels are carried out (Fig. 1). Endothermic peaks appear at 100 °C in the DSC curves which presumably are induced by the vaporization of absorbed water. The mass losses of the samples from 200 °C to 600 °C, shown on the TG curves, derive from the decompositions of the residual oxidizer (nitrates) and the organics (i.e. citric acid, tartaric acid, glycine or EDTA) in the precursor, resulting apparent exothermic peaks on the corresponding DSC curves [30]. Hereinto, the precursors with citric acid decompose in two exothermic steps at 431.6 °C and 476.7 °C with a total weight loss of 57% (Fig. 1(a)). This is very similar to Li' reports [28]. The first

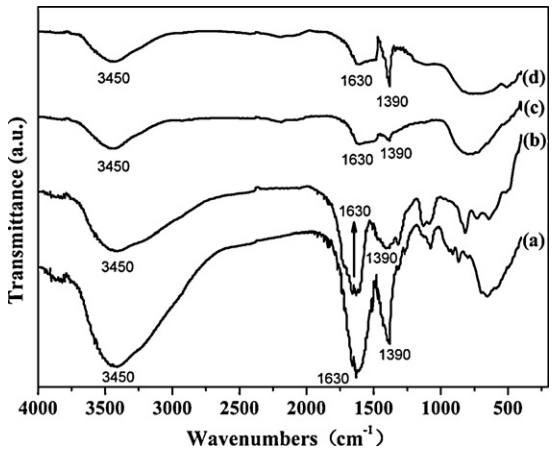

Fig. 2. IR spectra of the precursors: (a) citric acid; (b) tartaric acid; (c) glycine and (d) EDTA.

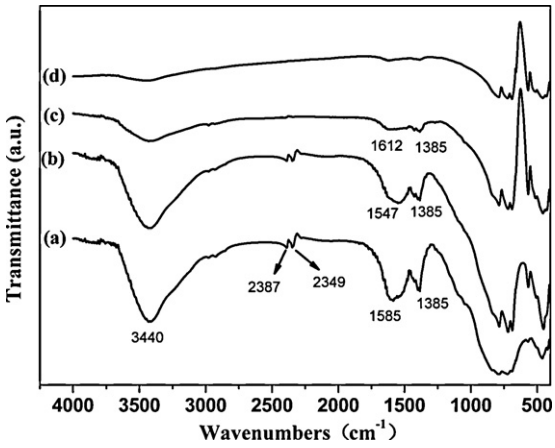

Fig. 3. IR spectra of the samples with EDTA calcined at various temperatures: (a) 750 °C; (b) 800 °C; (c) 850 °C and (d) 1000 °C.

thermally transformation induces by the further combustion process between the nitrates and citric acid, and the second step is the pyrolysis of the remnant organic at higher temperatures. However, the two well defined thermal events are not observed in other reactions because they appear to occur simultaneously. Precursors with EDTA, Fig. 1(d), exhibit the largest exothermic peak width (ranges from 300 °C to 600 °C), suggesting that the reaction between EDTA and nitrate occurs at a longer speed, while precursors with tartaric acid, Fig. 1(b), show the smallest exothermic peak width (ranges from 400 °C to 500 °C), possibly resulting from a fast reaction. During this process, CO_2, H_2O and NO_x gases maybe released. Two weak exothermic peaks at 858.8 °C and 916.4 °C for critic acid (Fig. 1(a)), could be attributed to the crystallization peak of amorphous YAG for the former and the oxidation of free carbon impurities for the latter [16]. Similar crystallization temperatures are observed in other systems, but the exothermic peaks appear at 886.0 °C and 945.6 °C, 901 °C and 951.4 °C, and 870.8 °C and 1036.8 °C in Fig. 1(b)–(d), respectively. Therefore, YAG nano-powders can be obtained by calcinations of the precursors in the range of 850–950 °C with various chelating agents and fuels.

3.2. Infrared spectra analyses

Fig. 2 gives the IR spectra of the same precursors. The broad bands centered at 3450 cm^{-1} in the spectra are characteristic O–H stretching vibrations of absorbed H_2O. Peaks localized at 1630 cm^{-1} and 1390 cm^{-1} can be assigned to the stretching vibration of carboxylate (O–C–O) and nitrate (O–N–O), respectively, indicating that the SHS process is incomplete [28,29]. The residuals cause apparent exothermic peaks in the DSC curves. No well-resolution peaks in the range 800–450 cm^{-1}, which are the characteristic Al–O and Y–O vibration, can be detected. It is concluded that the precursors are all amorphous. The above investigations of IR spectra demonstrate that the amorphous precursors have nearly the same composition.

Fig. 3 shows the IR spectra of samples prepared with EDTA calcined at various temperatures. Comparing to the spectra of precursors (Fig. 2(d)), two weak peaks localized at 2387 cm^{-1} and 2349 cm^{-1} in the spectra of the powder calcined at 750 °C are observed, caused by the trapped CO_2. The carboxylate (O–C–O) of the precursors transforms into the carbonate at 750 °C since the characteristic vibration shifts to 1585 cm^{-1}. For the powders calcined at 800 °C, the characteristic Al–O and Y–O vibration appears, revealing that the YAG phase has formed. It is consistent with the DSC results in addition to a small lag of crystallite temperature.

3.3. Phase analyses and size calculation by XRD

The XRD patterns of the powders calcined at 1000 °C for 2 h using different chelating agents and fuels are shown in Fig. 4. It can be seen that all diffraction lines conform to the cubic YAG phase (JCPDS No. 82-0575) and no impurity phases such as YAM ($Y_2Al_4O_9$) or YAP ($YAlO_3$) are observed. The high and sharp peaks are associated with the grain size of the YAG crystallites. Crystallite size of the powders calcined at 1000 °C can be determined by X-ray line broadening and calculated through the Scherrer equation:

$$d_{Crys} = \frac{0.89\lambda}{B\cos\theta}$$

where $B = (B_0^2 - B_c^2)^{1/2}$, B_0 is the full width at half maximum (in 2θ (°)), B_c is correction factor for instrument broadening, θ is the peak maximum (in 2θ (°)), and λ is the Cu $K_{\alpha 1}$ weighted average wavelength (λ = 1.54056 Å). The crystallite size calculated from the diffraction peak of the (4 2 0) crystal face is 63 nm, 68 nm, 49 nm and 36 nm for citric acid, tartaric acid, glycine and EDTA, respectively, as chelating agents and fuels. In view of the TG–DSC results, it can be established that particle sizes are closely related to the chelating agents and fuels which play an important role on the rate of combustion reaction.

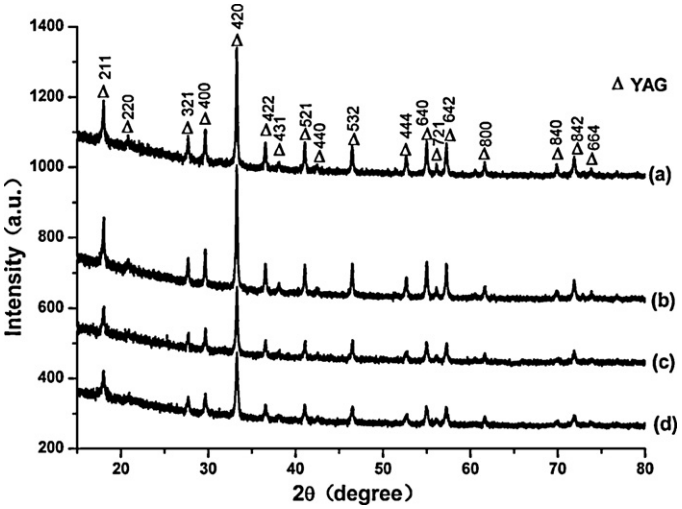

Fig. 4. The XRD patterns of the powders calcined at 1000 °C with (a) citric acid; (b) tartaric acid; (c) glycine and (d) EDTA.

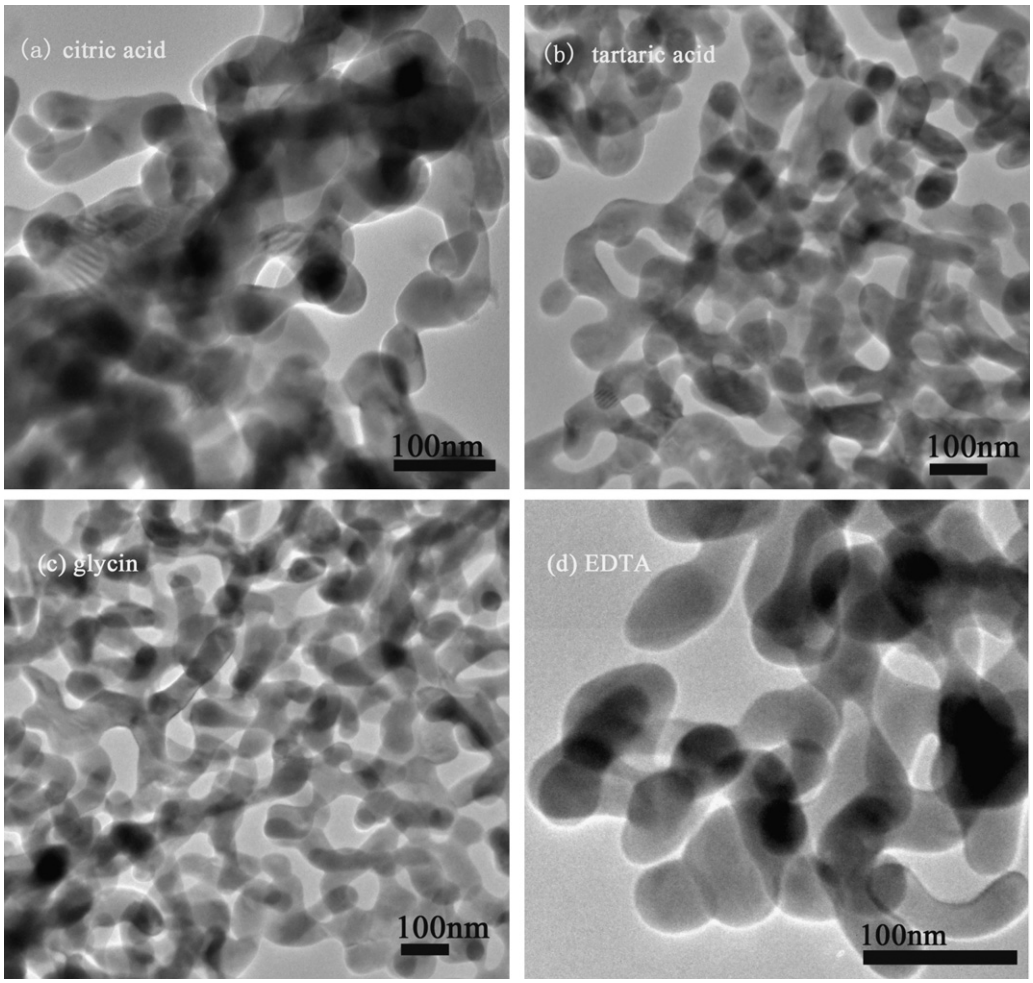

Fig. 5. The TEM micrographs of YAG using (a) citric acid; (b) tartaric acid; (c) glycine and (d) EDTA.

3.4. TEM and SEM studies

TEM analyses were carried out to further investigate about the morphology of YAG nano-powders. Fig. 5 shows the agglomerate structures of the YAG products calcined at 1000 °C. Most particles are semispherical in shape with significant porosity. Such porosity may result from the release of gas in the combustion process. By varying the organic, various specific surface areas can be obtained, which is confirmed by the adsorption and desorption of nitrogen test. As observed, the average size of nano-powders is about 60 nm, 80 nm, 60 nm and 40 nm when citric acid, tartaric acid, glycine and EDTA as chelating agents and fuels, respectively, reversed indicating that the chelating agents and fuels have a determining influence on the size and agglomeration of YAG nano-particles. Specifically, citric acid and tartaric acid that show the faster reaction, lead to larger average particle size. On the other hand, the smaller grains

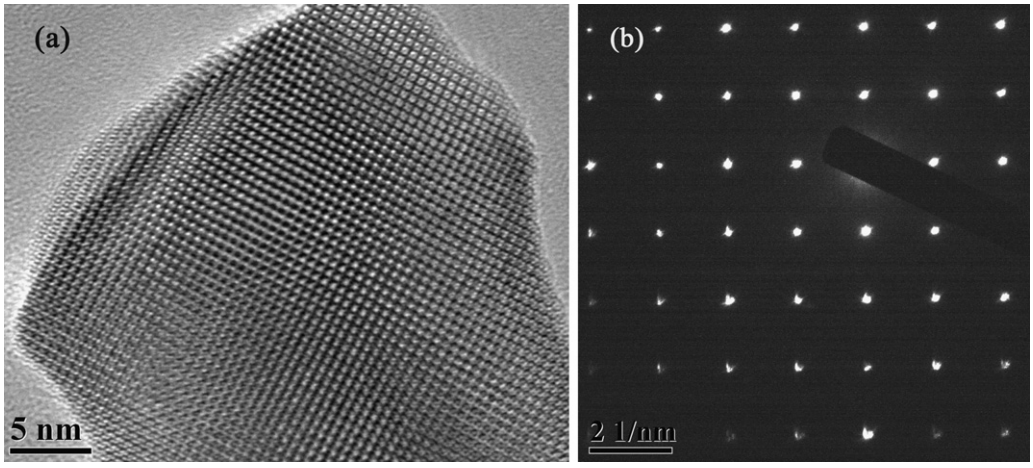

Fig. 6. The HRTEM and electron diffraction micrographs of YAG using EDTA calcined at 1000 °C.

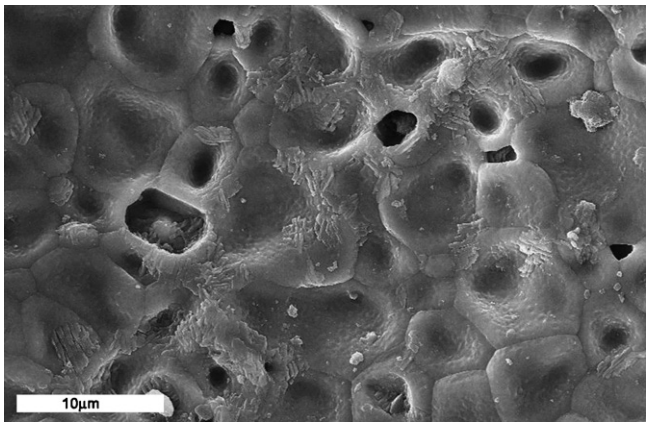

Fig. 7. The surface of YAG ceramics prepared with EDTA calcined at 1750 °C for 10 h.

are obtained when using EDTA. That is, the faster reaction means the fewer residues in synthesis process, which make the cations to diffuse more smoothly. Hence, utilizing a chelating agent with a high combustion reaction rate, results in average particle size larger than 60 nm owing to the smooth diffusion path for the cations. It induces the reduction of the sinterability. In addition, HRTEM measurement shows that YAG nano-powders calcined at 1000 °C are well crystallized. The average particle size is 30–40 nm when using EDTA (Fig. 6), which could be beneficial for the preparation of transparent YAG ceramics.

The SEM image recorded for YAG ceramics (EDTA, 1750 °C/10 h) is shown in Fig. 7. Some micro-scale pores can be observed in the ceramics. The grain size is 5–10 μm, which is smaller than the grain size of Nd:YAG ceramics prepared by starting material in bulk form at the same temperature [4], revealing that the grain boundaries can be controlled significantly by nano-powders.

4. Conclusions

Yttrium aluminum garnet nano-powders have been successfully synthesized by a sol–gel combustion method. The route involved various chelating agents and fuels, namely citric acid, tartaric acid, glycine and EDTA. Thermal decomposition of organics-nitrate gel leads to amorphous precursors that later transformed into pure YAG nano-powders by calcination at 1000 °C. The effect of the chelating agents and fuels on the particle size and agglomeration was investigated and the results showed that the faster reaction, the smaller size of particles generated. By using EDTA, the smallest size particles were obtained caused probably by a significant blocking of diffusion path associated with the lowest combustion reaction rate. The fabrication of transparent YAG ceramics using the nano-powders made with EDTA precursors is under way among the research endeavors in our laboratory.

Acknowledgments

We would like to acknowledge the support from National Natural Science Foundation of China (Grant No. 50990304) and the Major Basic Research Programme of Shanghai (Grant No. 07DJ14001). Dr. Xiangxin Guo thanks financial supports from the "Hundred Talent Project" of Chinese Academy of Sciences and the "Pujiang Talent Project" of Shanghai Sciences and Technology Committee (Grant No. 09PJ1410600). We also appreciate very much of the suggestions associated with this work from Dr. E. Alejandro Leon-Escamilla from the Universidad Politécnica de Valencia (Spain).

References

[1] P. Lacovara, H.K. Choi, C.A. Wang, R.L. Aggarwal, T.Y. Fan, Opt. Lett. 16 (1991) 1089–1091.
[2] S.K. Ruan, J.G. Zhou, A.M. Zhong, J.F. Duan, X.B. Yang, M.Z. Su, J. Alloys Compd. 275 (1998) 72–75.
[3] E. Caponetti, D.C. Martino, M.L. Saladino, C. Leonelli, Langmuir 23 (2007) 3947–3952.
[4] A. Ikesue, T. Kinoshita, K. Kamata, K. Yoshida, J. Am. Ceram. Soc. 78 (1995) 1033–1040.
[5] L.B. Kong, J. Ma, H. Huang, Mater. Lett. 56 (2002) 344–348.
[6] S.H. Lee, S. Kochawattana, G.L. Messing, J.Q. Dumm, G. Quarles, V. Castillo, J. Am. Ceram. Soc. 89 (2006) 1945–1950.
[7] M.S. Tsai, W.C. Fu, W.C. Wu, C.H. Chen, C.H. Yang, J. Alloys Compd. 455 (2008) 461–464.
[8] M. Nyman, J. Caruso, M.J. Hampden-Smith, T.T. Kodas, J. Am. Ceram. Soc. 80 (1997) 1231–1238.
[9] M. Veith, S. Mathur, A. Kareiva, M. Jilavi, M. Zimmer, V. Huch, J. Mater. Chem. 9 (1999) 3069–3079.
[10] A. Leleckaite, A. Kareiva, Opt. Mater. 26 (2004) 123–128.
[11] N. Matsushita, N. Tsuchiya, K. Nakatsuka, T. Yanagitani, J. Am. Ceram. Soc. 82 (1999) 1977–1984.
[12] E. Caponetti, M.L. Saladino, F. Serra, S. Enzo, J. Mater. Sci. 42 (2007) 4418–4427.
[13] J. Su, Q.L. Zhang, S.F. Shao, W.P. Liu, S.M. Wan, S.T. Yin, J. Alloys Compd. 470 (2009) 306–310.
[14] J. Marchal, T. Johns, R. Baranwal, T. Hinklin, R.M. Laine, Chem. Mater. 16 (2004) 822–831.
[15] S. Ramanathan, M.B. Kakade, S.K. Roy, K.K. Kutty, Ceram. Int. 29 (2003) 477–484.
[16] F.G. Qiu, X.P. Pu, R. Zhang, J.K. Guo, Key Eng. Mater. 280 (2005) 717–719.
[17] S. Tsao, Y.P. Fu, C.T. Hu, J. Alloys Compd. 419 (2006) 197–200.
[18] J. Li, Y. Pan, F. Qiu, Y. Wu, J. Guo, Ceram. Int. 34 (2008) 141–149.
[19] L. Yang, T. Lu, H. Xu, N. Wei, J. Alloys Compd. 484 (2009) 449–451.
[20] M.P. Pechini, Method of preparing lead and alkaline earth titanate and niobates and coating method using the same to form a capacitor [P]. US: 3330697, 1967.
[21] N. Zhou, G. Chen, H.Z. Xian, H.J. Zhang, Mater. Res. Bull. 43 (2008) 2554–2562.
[22] B.G. Toksha, S.E. Shirsath, S.M. Patange, K.M. Jadhav, Solid State Commun. 147 (2008) 479–483.
[23] K. Nagaveni, G. Sivalingam, M.S. Hedge, G. Madras, Appl. Catal. B: Environ. 48 (2004) 83–93.
[24] Y. Huang, Y. Tang, J. Wang, Q. Chen, Mater. Chem. Phys. 97 (2006) 394–397.
[25] A.K. Pradhan, K. Zhang, G.B. Loutts, Mater. Res. Bull. 39 (2004) 1291–1298.
[26] T. Tachiwaki, M. Yoshinaka, K. Hirota, T. Ikegami, O. Yamaguchi, Solid State Commun. 119 (2001) 603–606.
[27] X. Li, Q. Li, J. Wang, S. Yang, H. Liu, Opt. Mater. 29 (2007) 528–531.
[28] J. Li, Y. Pan, F. Qiu, Y. Wu, W. Liu, J. Guo, Ceram. Int. 33 (2007) 1047–1052.
[29] R.V. Mangalaraja, J. Mouzon, P. Hedström, I. Kero, K.V.S. Ramam, C.P. Camurri, M. Odén, J. Mater. Process Technol. 208 (2008) 415–422.
[30] A.L. Costa, L. Esposito, V. Medri, A. Bellosi, Adv. Eng. Mater. 9 (2007) 307–312.